Acta Biochim Biophys Sin (2008): 194-201 | © 2008 Institute of Biochemistry and Cell Biology, SIBS, CAS | All Rights Reserved 1672-9145
http://www.abbs.info; www.blackwellpublishing.com/abbs | DOI: 10.1111/j.1745-7270.2008.00393.x

Class I phosphatidylinositol 3-kinase inhibitor LY294002 activates autophagy and induces apoptosis through p53 pathway in gastric cancer cell line SGC7901

Chungen Xing[1], Baosong Zhu[1]*, Huihui Liu[2], Huihua Yao[1], and Lifeng Zhang[3]

[1] Department of General Surgery, The Second Affiliated Hospital, Soochow University, Suzhou 215004, China
[2] Department of Neurology, The Second Affiliated Hospital, Soochow University, Suzhou 215004, China
[3] Soochow University School of Medicine, Suzhou 215123, China

We aimed to study the effects of LY294002, an inhibitor of class I phosphatidylinositol 3-kinase (PI3K), on proliferation, apoptosis, and autophagy in gastric cancer cell line SGC7901. In this study, we showed that LY294002 inhibited the viability of gastric cancer SGC7901 cells. We also showed that LY294002 increased the expression of microtubule-associated protein 1 light chain 3 (LC3), and increased monodansylcadaverine (MDC)-labeled vesicles. LY294002 activated autophagy by activating p53 and caspase-3, and induced apoptosis by up-regulating *p53* and p53-up-regulated modulator of apoptosis (*PUMA*). Therefore, LY294002 might induce cytotoxicity in SGC7901 cells through activation of *p53* and the downstream point *PUMA*. These findings suggest that inhibition of the class I PI3K signaling pathway is a potential strategy for managing gastric cancers.

Keywords PI3K; LY294002; autophagy; apoptosis

The class I phosphatidylinositol 3-kinase (PI3K) pathway plays a central role in the regulation of cell proliferation, growth, differentiation, and survival [1,2]. Dysregulation of this pathway is frequently observed in a variety of tumors, including brain tumors, breast, ovarian, and other carcinomas [3–5]. Therefore, inhibition of PI3K signaling is being investigated as a potential therapy for cancer.

In mammalian cells, there are three classes of PI3Ks, class I, class II, and class III. Class I and class III PI3K regulate autophagy differently. The class I PI3K/serine-threonine protein kinase (AKT)/mammalian target of rapamycin (mTOR) signal, which is activated in cancer cells through the growth factor receptor, inhibits autophagy [6]. Contradictorily, class III PI3K promotes the sequestration of cytoplasmic material that occurs during autophagy. Class II PI3K activity is thought to have no relevance to the autophagy control [7].

Autophagy has been shown to prolong cell survival under physiologic, pathologic, and pharmacologic stress conditions [8,9]. Deregulation of autophagy is associated with liver diseases, neurodegenerative diseases, cardiomyopathies, and cancers [8,10]. Furthermore, like apoptosis, autophagy is found to be suppressed in malignant tumors and in tumorigenesis. Several molecular and cell signaling pathways have been implicated in regulating autophagy, such as Beclin1, death-associated protein kinase, death-associated related protein kinase 1, mitogen-activated kinase, and PI3K/AKT/mTOR pathways [11–13].

Recent studies have shown that the inhibition of class I PI3K/AKT and its downstream target mTOR contributes to the initiation of autophagy [14,15]. Therefore, the inhibitor of class I PI3K/AKT/mTOR signaling has emerged as an important and attractive therapeutic target for cancer therapy. However, detailed mechanisms of the relation between apoptosis, autophagy, and necrosis in programmed cell death (PCD) are poorly understood.

Materials and Methods

Drug preparation

LY294002 (Cell Signaling Technology, Beverly, USA) was diluted in DMSO to create a stock solution that was stored

Received: August 22, 2007 Accepted: January 3, 2008
This work was supported by a grant from the Health Foundation of Jiangsu Province (H200719)
Corresponding author: Tel/Fax, 86-512-67783997; E-mail, baosongzhu@yahoo.com.cn

according to the manufacturer's suggestions. The final solution used in the experiments was 50 μM. This concentration of LY294002 was selected on the basis of our experiments on SGC7901 cells.

Cell culture

SGC7901 gastric cancer cells (Shanghai Institute of Cell Biology, Shanghai, China) were maintained in RPMI 1640 medium (Gibco BRL, Rockville, USA) containing 10% heat-inactivated fetal bovine serum (FBS; Hangzhou Sijiqing Biological Engineering Material Company Limited, Hangzhou, China), 0.03% L-glutamine (Sigma, St. Louis, USA) and incubated in a 5% CO_2 atmosphere at 37 ºC. Cells in mid-log phase were used in experiments.

Cell viability assay

Cell viability was assessed by 3-[4,5-dimethylthiazol-2-yl]-2,5-diphenyltetrazolium bromide (MTT; Sigma) assay. To determine the time-course of the effects of LY294002 on SGC7901 cells, cells were plated into 96-well microplates (7×10^3 cells/well) and cultured for 24, 48, and or 72 h. Then LY294002 (12.5 μM, 25 μM, or 50 μM) was added to the culture medium and cell viability was assessed with MTT at 24, 48, and 72 h after drug treatment. Later, MTT solution was added to the culture medium (500 μg/ml of final concentration) 4 h before the end of treatment and the reaction was stopped by addition of 100 μl of 10% acidic sodium dodecyl sulfate. The absorbance value (*A*) at 570 nm was read using an automatic multiwell spectrophotometer (Bio-Rad, Richmond, USA). The percentage of cell death was calculated as following equation:

$$\text{Cell death rate}=(1-A_{\text{experiment group}}/A_{\text{positive control}})\times100\%$$

Hoechst 33258 staining

After treatment, cell cultures were washed twice with phosphate-buffered saline (PBS) and incubated with 2 μM Hoechst 33258 (Beyotime, Nantong, China) for 1 h in the dark at 37 ºC. After washing three times with PBS, the cells were viewed with a fluorescence microscope (Nikon, Tokyo, Japan) equipped with an ultraviolet filter. The images were recorded on a computer with a digital camera (DXM 1200; Nikon) attached to the microscope, and the images were processed by computer. The Hoechst reagent was taken up by the nuclei of the cells, and apoptotic cells showed a bright blue fluorescence.

Visualization of monodansylcadaverine (MDC)-labeled vacuoles

Exponentially growing cells were plated on 24-chamber culture slides, cultured for 24 h, then incubated with LY294002 in RPMI 1640 medium containing 10% FBS for 6 h, 12 h, or 24 h. Autophagic vacuoles were labeled with MDC [16] (Sigma) by incubating cells with 1 μM MDC in RPMI 1640 at 37 ºC for 10 min. After incubation, cells were washed three times with PBS and immediately analyzed with a fluorescence microscope (Eclipse TE 300; Nikon) equipped with a filter system (V-2A; excitation filter, 380–420 nm; barrier filter, 450 nm). Images were captured with a CCD camera and imported into Photoshop CS2 (Adobe, San Jose, USA).

Detection and quantification of acidic vesicular organelles with acridine orange (AO)

Vital staining of cells with AO (KeyGEN, Nanjing, China) was carried out essentially as described previously [17]. Exponentially growing cells were plated on 24-chamber culture slides, cultured for 24 h, then incubated with LY294002 in RPMI 1640 containing 10% FBS for 6, 12, or 24 h. AO was added for 15 min at a final concentration of 1 μg/ml, and the cells were then washed three times with PBS. Unfixed cells were examined immediately by fluorescence microscopy using a Nikon Eclipse 300 microscope with the red filter set (G-2E/C; excitation 528–553 nm, emission 600–660 nm). Red fluorescence was observed with excitation and emission wavelengths set at 488 nm and 655 nm, respectively. Images were captured with a CCD camera and imported into Photoshop.

Immunofluorescence staining

SGC7901 cells were seeded onto 24-chamber culture slides and treated with LY294002 (50 μM). After fixation (methanol) for 10 min and blockage (1% bovine serum albumin solved in 0.1% Triton X-100) for 1 h, cells were incubated with rabbit monoclonal primary antibody against active caspase-3, mouse monoclonal primary antibody against p53, or rabbit monoclonal primary antibody against p53-up-regulated modulator of apoptosis (PUMA) (Cell Signaling Technology) diluted 1:200 with PBS containing 1% bovine serum albumin at 4 ºC overnight. Cells were then incubated for 1 h with 1:500 CY3-conjugated sheep anti-rabbit secondary antibody (Sigma) or FITC-conjugated rabbit anti-mouse secondary antibody (Sigma) to visualize the binding sites of the primary antibody under laser confocal microscopy (Leica, Bensheim, Germany).

Real-time quantitative RT-PCR analysis of microtubule-associated protein 1 light chain 3 (*LC3*)

Total RNA was extracted with the RNAiso reagent kit

(TaKaRa, Dalian, China). First-strand cDNA was generated by RT of 2 μg total RNA using random primers and Primescript™ RT reagent kit (TaKaRa), according to the manufacturer's instructions, in a total reaction volume of 20 μl. The sequences of forward and reverse oligonucleotide primers, specific to the chosen candidate and housekeeping genes, were designed using Primer5 software (http://frodo.wi.mit.edu/cgi-bin/primer5/primer5_www.cgi). The primers for *LC3* were 5′-CTTGGATTGGTGGGATGTTC-3′ (forward) and 5′-GATGATGGACTGTAGGAGCGTGT-3′ (reverse), GenBank accession No. NM_018370, nucleotides, 758–870. The primers for β-actin were 5′-ATTGCCGACAGGATGCAGA-3′ (forward) and 5′-GAGTACTTGCGCTCAGGAGGA-3′ (reverse), GenBank accession No. NM_001101, nucleotides, 998–1086. Real-time quantitative PCR was also carried out in an iCycler 5 iQ real-time PCR system (Bio-Rad). An 80-fold dilution of each cDNA was amplified in a 20 μl volume, using the SYBR Premix EX Taq kit (TaKaRa), with 500 nM final concentrations of each primer. The amplification specificity was checked by melting curve analysis. Threshold cycle Ct, which correlates inversely with the target mRNA levels, was calculated using the second derivative maximum algorithm provided by LightCycler software (Bio-Rad). For each cDNA, the LC3 mRNA levels were normalized to β-actin mRNA levels. Results are expressed as the ratio of normalized LC3 mRNA levels of treated cells to that of untreated cells.

Western blot analysis

Cells were harvested and rinsed twice with ice-cold PBS. Five volumes of Western blot lysis buffer [10 mM Tris-HCl (pH 7.4), 150 mM NaCl, 1% Triton X-100, 1% sodium deoxycholate, 0.1% sodium dodecyl sulfate, 5 mM EDTA, 1 mM phenylmethylsulphonyl fluoride, 0.28 μg/ml aprotinin, 50 μg/ml leupeptin, 1 mM benzamidine, and 7 μg/ml pepstatin A] for each volume of cell pellets was added and the mixture was sonicated on ice (1 s/ml per sonicate, waiting 30 s between intervals, carried out five times). The mixture was microcentrifuged at 10,600 *g* at 4 ºC for 10 min and the supernatant was preserved at –70 ºC for later use. Protein concentration was determined with a BCA kit (Pierce, Rockford, USA). Proteins were separated by 12% sodium SDS-PAGE gel, transferred to a nitrocellulose membrane, and immunoblotted with primary antibody 1:500 (Cell Signaling Technology) at 4 ºC overnight. The immunoreactivites were detected using horseradish peroxidase-conjugated anti-rabbit antibody (Sigma) used 1:5000 in blocking solution for 1 h at room temperature. Immunoreactivity was detected with an enhanced chemiluminescence kit (Amersham Pharmacia Biotech, Piscataway, USA) and visualized by autoradiography. Protein β-actin (Sigma) was used as the loading control.

Statistical analysis

All data are presented as the mean±SD. Statistical analysis was carried out by ANOVA followed by Dunnett's *t*-test, considering $P<0.05$ as significant.

Results

Cell viability was inhibited after LY29400 treatment

LY294002 inhibited SGC7901 viability in a dose-dependent and time-dependent fashion. MTT assays revealed that, after 24 h of treatment, the rate of inhibition reached 20.71%±4.13% at the highest dose of 50 μM, and after 48 h of treatment the rate of inhibition was found to be approximately 41.54%±2.06%. When the incubation time was prolonged to 72 h, the inhibition rate rose to 64.09%±1.65% (**Fig. 1**).

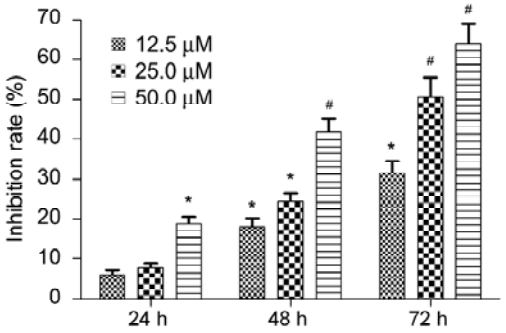

Fig. 1 Reduced viability of gastric cancer SGC7901 cells after LY294002 treatment SGC7901 cells (7×10^4 cells/ml) were cultured with various doses of LY294002 for the indicated times and cell viability was analyzed by MTT assay. Values given are the mean±SD of three independent experiments. *$P<0.05$ compared to control; # $P<0.01$ compared to control.

Apoptosis was induced in SGC7901 cells after LY294002 treatment

Treatment with 50 μM LY294002 for 6, 12, or 24 h in SGC7901 cells produced intense Hoechst-positive staining of condensed nuclei, indicative of apoptosis. Significant increase in Hoechst staining was observed along with apoptosis when cells were treated with 50 μM LY294002. We also used immunofluorescence staining for activated caspase-3 to detect apoptotic conditions after treatment

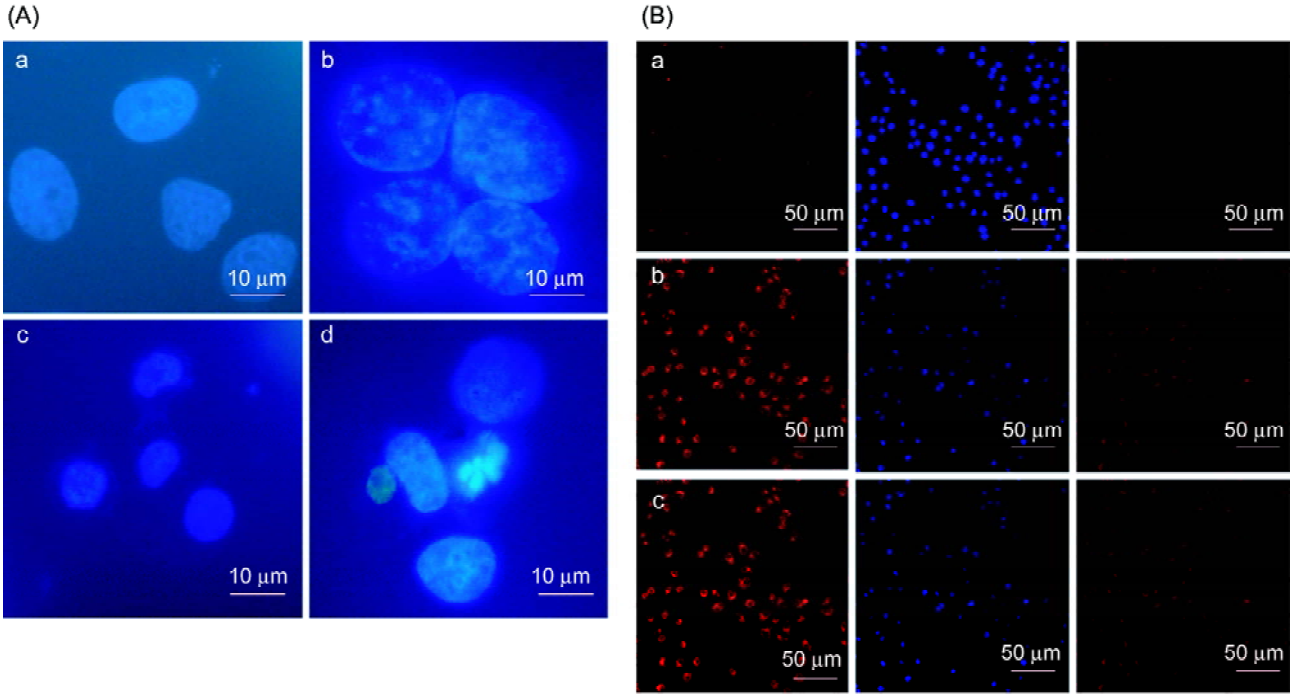

Fig. 2 Apoptosis was induced in gastric cancer SGC7901 cells after treatment with LY294002 (A) Hoechst 33258 staining showed apoptosis was induced after SGC7901 cells were incubated with LY294002 (50 μM) for 6 h (b), 12 h (c), or 24 h (d), and then stained with Hoechst 33258 (10 mM). (a) The control. (B) Activated caspase-3 expression and distribution in SGC7901 cells after treatment with LY294002. Cells were treated with LY294002 (50 μM) for 12 h (b) or 24 h (c) and analyzed by immunofluorescence microscopy using activated caspase-3 antibodies. (a) The control. Fluorescence particles with red showed apoptosis. LY294002 increased the distribution of activated caspase-3 from 12 h to 24 h.

with LY294002. The activation of caspase-3 signifies the beginning of apoptosis. All the results indicated that LY294002 induced apoptosis (**Fig. 2**).

LY294002 increased autophagic vacuoles

The autofluorescent substance MDC has been shown to be a marker for late autophagic vacuoles but not endosomes [16]. The dye is trapped in acidic, membrane-rich organelles and also shows increased fluorescence quantum yield in response to the compacted lipid bilayers present in late autophagic vacuoles [18]. When cells are viewed with a fluorescence microscope, autophagic vacuoles stained by MDC appear as distinct dot-like structures distributed within the cytoplasm or localizing in the perinuclear regions. We found that there was an increase in the number of MDC-labeled vesicles after treatment with LY294002 from 6 to 24 h (**Fig. 3**).

LY294002 increased acidic vesicular organelles

The maturation of autophagosomes to autolysosomes is accompanied by an increase in the acidity of the lumen [20]. Therefore, to assess the relative number of autolysosomes in control versus LY294002-treated cells, we used an assay that measures supravital staining of acidic compartments with the lysosomotropic agent AO. When the dye enters an acidic compartment, the protonated form becomes trapped in aggregates that fluoresce bright red or orange [20–22]. Although AO stains lysosomal and late endosomal compartments as well as autolysosomes, extensive studies have established that a substantial increase in AO-positive acidic vesicular organelles also occurs in conjunction with the induction of macroautophagy in glioblastoma cells [14,22–24]. As shown in **Fig. 4**, a general increase in the intensity of AO-positive structures could be detected in LY294002-treated cells, but not in the control cells. The results confirmed that LY294002 treatment stimulates a large increase in the amount of AO sequestered into acidic vesicular organelles.

LY294002 up-regulated expression of *LC3* mRNA

To assay if LY294002 increases the expression of autophagic genes, real-time quantitative RT-PCR analysis

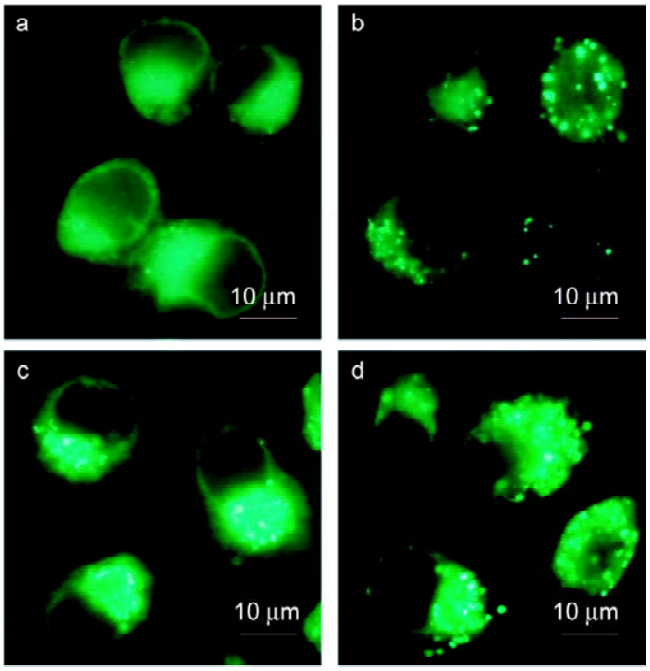

Fig. 3 Monodansylcadaverine (MDC) staining shows autophagy was activated in gastric cancer SGC7901 cells after treatment with LY294002 SGC7901 cells were incubated with LY294002 (50 μM) for 6 h (b), 12 h (c), 24 h (d) and then stained with MDC (100 μM). (a) The control. Fluorescence particles with green dots show late autophagic vacuoles.

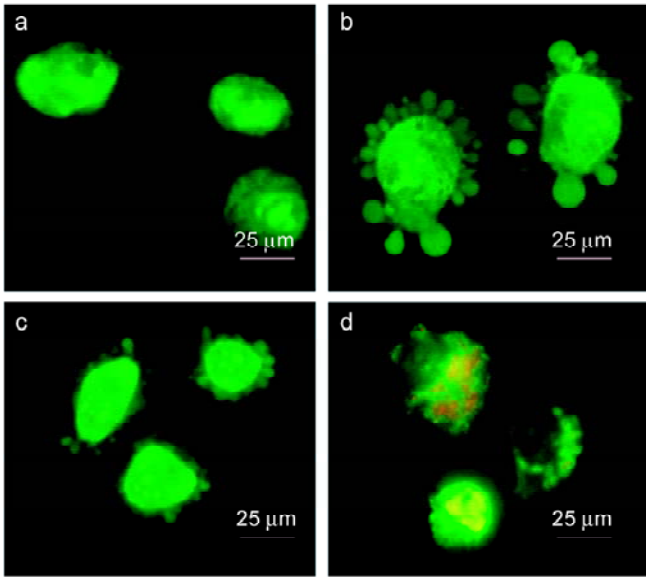

Fig. 4 Acridine orange (AO) staining shows acidic vesicular organelles were activated after gastric cancer SGC7901 cells were treated with LY294002 SGC7901 cells were incubated with LY294002 (50 μM) for 6 h (b), 12 h (c), 24 h (d), and then stained with AO (1 μg/ml). (a) The control. Fluorescence particles with green dots show acidic vesicular organelles.

was used to detect the expression of *LC3*. The results showed that the basal level of *LC3* mRNA in SGC7901 cells was low. After incubation with LY294002, the *LC3* mRNA expression was significantly increased after 6 h (**Fig. 5**).

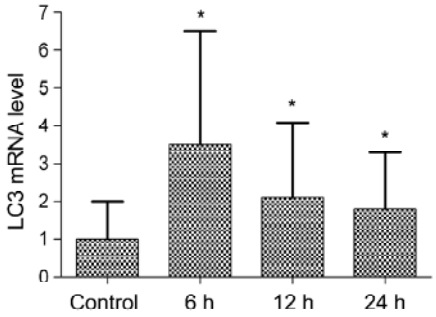

Fig. 5 Real-time quantitative RT-PCR analysis of the autophagic gene *LC3* of control gastric cancer SGC7901 cells and SGC7901 cells treated with LY294002 Cells were treated with LY294002 (50 μM) for the indicated times. Values given are the mean±SD of three independent experiments. Statistical analysis was carried out with ANOVA followed by Student's *t*-test. **P*<0.05 compared to control.

LY294002 increased expression of p53 and PUMA

The tumor suppressor and nuclear transcription factor p53 is a tetramer phosphoprotein that can regulate several major cellular functions including gene transcription, DNA synthesis, DNA repair, cell cycle regulation, senescence, and cell death [25,26]. p53 is activated by cell stress and DNA damage and, depending on the severity of the stress and the particular cell type, might aid in adaptive responses to the stress, or trigger cell cycle arrest or apoptosis [27]. When the inhibitor of class I PI3K, LY294002, was applied, the autophagic level was significantly increased and the apoptotic level was increased, indicating that class I PI3K is a key regulator of both autophagy and apoptosis. In addition, when p53 was activated by LY294002, the level of autophagy was up-regulated, indicating that p53 is relevant to autophagy and apoptosis and p53 activation increased autophagy levels, and at the same time, the apoptotic was induced (**Fig. 6**).

PUMA is a downstream target of the p53 tumor suppressor gene and a member of the BH3-only group of Bcl-2 family proteins [28,29]. The activation of PUMA by DNA damage is dependent on p53 and is mediated by the direct binding of p53 to the PUMA promoter region [30]. PUMA plays an essential role in p53-dependent and

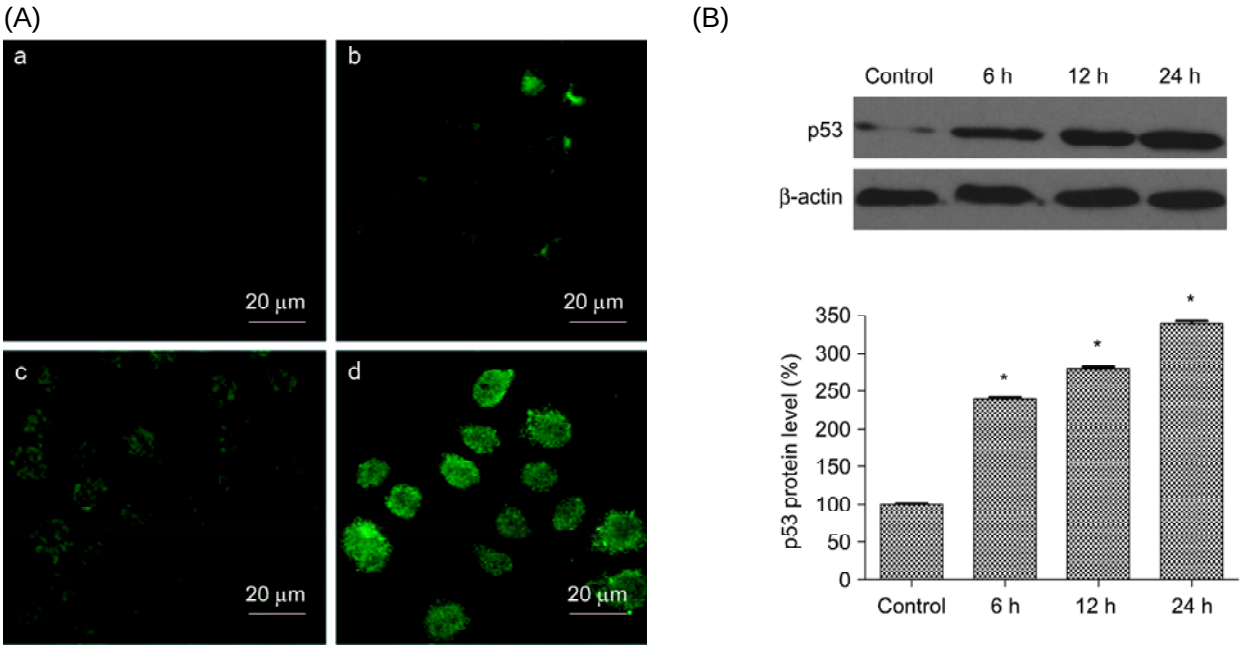

Fig. 6 p53 expression and distribution in gastric cancer SGC7901 cells after treatment with LY294002 (A) p53 expression and distribution in SGC7901 cells after treatment with LY294002. Cells were treated with LY294002 (50 μM) for 6 h (b), 12 h (c), or 24 h (d) and analyzed with an immunofluorescence microscope using p53 antibody. (a) The control. LY294002 increased the distribution of p53 from 6 to 24 h. (B) Increased expression of p53 after LY294002 exposure. SGC7901 cells were treated with LY294002 (50 μM) for 6 h, 12 h or 24 h. Western blot analysis was carried out on lysates from control and LY294002-treated cells to detect the protein levels of p53 (top panel). Quantitative analysis of p53 protein levels was also carried out (bottom panel). Values given are the mean±SD of three independent experiments. The results indicated that LY294002 up-regulated the protein expression of p53. Statistical comparisons were carried out with Dunnett's *t*-test. **P*<0.05 versus control.

p53-independent apoptosis induced by a variety of stimuli [30]. In this study, using the inhibitor of class I PI3K, LY294002, p53 was activated and the MAP1-LC3 levels were up-regulated, with increased apoptosis and significantly increased expression of PUMA (**Fig. 7**).

Discussion

Autophagy is a genetically programmed, evolutionarily conserved process that degrades long-lived cellular proteins and organelles. Autophagy is important in normal development and response to changing environmental stimuli and, in addition to its role in cancer, is important in numerous diseases, including bacterial and viral infections, neurodegenerative disorders, and cardiovascular disease [11]. Recent studies have suggested that there are three types of PCD: apoptosis (PCD I); autophagic cell death (PCD II); and necrosis (PCD III) [31].

The relationship between autophagy and apoptosis is very complicated. Boya *et al* [32] hypothesized that autophagy is needed to prevent apoptosis as a cell survival mechanism. Edinger and Thompson [31] were of the opinion that autophagy activates apoptosis and necrosis as a beginning factor. Although there has been great progress in autophagy since 2003, the relationship between autophagy and apoptosis is still discussed.

LC3 is an autophagosomal ortholog of yeast Atg8. LC3 has been best characterized as an autophagosomal marker in mammalian autophagy, and the levels of *LC3* might also reflect the levels of autophagy [33]. Our results showed that the basal level of *LC3* mRNA in SGC7901 cells was low. After incubation with LY294002, the *LC3* mRNA expression was significantly increased after 6 h.

The tumor suppressor *p53* plays a central role in sensing various genotoxic stresses. Here, we showed that these two important cellular signaling pathways, p53 and class I PI3K/AKT/mTOR, communicate with each other. p53 activation by a physiologically relevant stress signal, DNA damage, inhibits mTOR activity in normal cells [34]. The inhibitor of mTOR might activate p53 and autophagy. Autophagy is a lysosome-dependent cellular degradative process that, in the extreme case, could lead to cell death

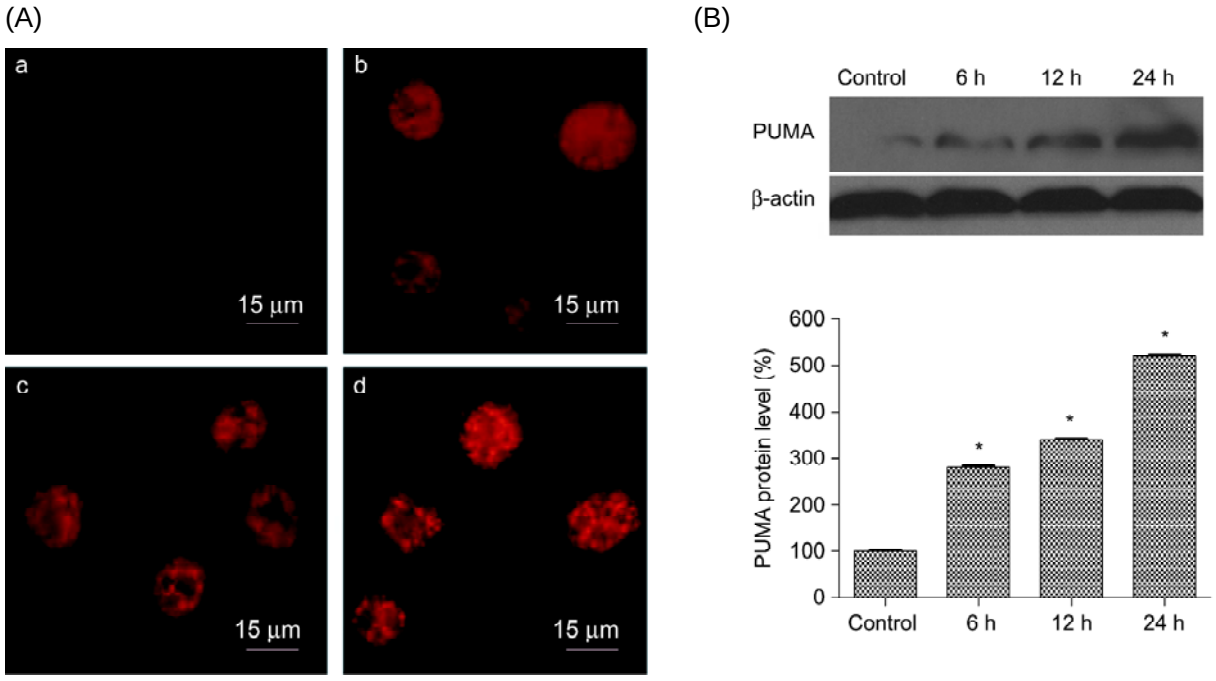

Fig. 7 p53-up-regulated modulator of apoptosis (PUMA) in gastric cancer SGC7901 cells after LY294002 treatment (A) Expression and localization of PUMA in SGC7901 cells after LY294002 treatment. Cells were treated with LY294002 (50 μM) for 6 h (b), 12 h (c), or 24 h (d) and analyzed by an immunofluorescence microscopy using PUMA antibody. (a) Basal control. (B) Increased expression of PUMA after LY294002 exposure (n=3). SGC7901 cells were treated with LY294002 (50 μM) for 6 h, 12 h, or 24 h. Western blot analysis was carried out on lysates from control and LY294002-treated cells to detect the protein levels of PUMA (top panel). Quantitative analysis of PUMA protein levels was also carried out (bottom panel). Values given are the mean±SD of three independent experiments. The results indicated that LY294002 up-regulated the expression of PUMA. Statistical comparisons were carried out with Dunnett's t-test. *P<0.05 versus control.

(PCD II). Autophagy appears to represent a unique tumor suppression mechanism. The activation of p53 dramatically increases autophagy levels in cells, perhaps contributing to the tumor suppressor functions of p53.

The results of activation of *p53* might rely on the autophagy and apoptosis levels and the relationship between autophagy and apoptosis. Low levels of *p53* activation and autophagy might promote cell proliferation and protect them against cell death, and when the levels of activation of *p53* extend to some degrees, it could induce cell death by activating p53 and autophagy.

In this study, when using the inhibitor of class I PI3K, LY294002, the level of *p53* and autophagy was activated. At the same time the expression of PUMA was up-regulated and the level of apoptosis and necrosis was increased. These results could prove the effects of class I PI3K/AKT/mTOR and p53 in regulating autophagy, apoptosis, and necrosis. All of these observations suggest that autophagy and p53 activation might have significant contributions to LY294002-induced death of SGC7901 cells. Further investigation of upstream signal regulation of autophagy and apoptosis could provide new insights into the mechanisms accommodating or contributing to autophagy and apoptosis, thereby unveiling new strategies for tumor therapy.

References

1 Vogt PK. PI 3-kinase, mTOR, protein synthesis and cancer. Trends Mol Med 2001, 7: 482–484
2 Oldham S, Hafen E. Insulin/IGF and target of rapamycin signaling: a TOR de force in growth control. Trends Cell Biol 2003, 13: 79–85
3 Choe G, Horvath S, Cloughesy TF, Grosby K, Seligson D, Palotie A, Inge L *et al*. Analysis of the phosphatidylinositol 3′-kinase signaling pathway in glioblastoma patients *in vivo*. Cancer Res 2003, 63: 2742–2746
4 Neve RM, Holbro T, Hynes NE. Distinct roles for phosphoinositide 3-kinase, mitogen-activated protein kinase and p38 MAPK in mediating cell cycle progression of breast cancer cells. Oncogene 2002, 21: 4567–4576
5 Philp AJ, Campbell IG, Leet C, Vincan E, Rockman SP, Whitehead RH, Thomas RJ *et al*. The phosphatidylinositol 3′-kinase p85alpha gene is an oncogene in human ovarian and colon tumors. Cancer

Res 2001, 61: 7426–7429
6 Arico S, Petiot A, Bauvy C, Dubbelhuis PF, Meijer AJ, Codogno P, Ogier-Denis E. The tumor suppressor PTEN positively regulates macroautophagy by inhibiting the phosphatidylinositol 3-kinase/protein kinase B pathway. J Biol Chem 2001, 276: 35243–35246
7 Tassa A, Roux MP, Attaix D, Bechet DM. Class III phosphoinositide 3-kinase-Beclin1 complex mediates the amino acid-dependent regulation of autophagy in C2C12 myotubes. Biochem J 2003, 376: 577–586
8 Kelekar A. Autophagy. Ann NY Acad Sci 2005, 1066: 259–271
9 Cuervo AM. Autophagy: in sickness and in health. Trends Cell Biol 2004, 14: 70–77
10 Gozuacik D, Kimchi A. Autophagy as a cell death and tumor suppressor mechanism. Oncogene 2004, 23: 2891–2906
11 Shintani T, Klionsky DJ. Autophagy in health and disease: a double-edged sword. Science 2004, 306: 990–995
12 Kondo Y, Kanzawa T, Sawaya R, Kondo S. The role of autophagy in cancer development and response to therapy. Nat Rev Cancer 2005, 5: 726–734
13 Petiot A, Ogier-Denis E, Blommaart EF, Meijer AJ, Codogno P. Distinct classes of phosphatidylinositol 3′-kinases are involved in signaling pathways that control macroautophagy in HT-29 cells. J Biol Chem 2000, 275: 992–998
14 Takeuchi H, Kondo Y, Fujiwara K, Kanzawa T, Aoki H, Mills GB, Kondo S. Synergistic augmentation of rapamycin-induced autophagy in malignant glioma cells by phosphatidylinositol 3-kinase/protein kinase B inhibitors. Cancer Res 2005, 65: 3336–3346
15 Paglin S, Lee NY, Nakar C, Fitzgerald M, Plotkin H, Deuel B, Hackett N *et al*. Rapamycin-sensitive pathway regulates mitochondrial membrane potential, autophagy, and survival in irradiated MCF-7 cells. Cancer Res 2005, 65: 11061–11070
16 Biederbick A, Kern HF, Elsasser HP. Monodansylcadaverine (MDC) is a specific *in vivo* marker for autophagic vacuoles. Eur J Cell Biol 1995, 66: 3–14
17 Paglin S, Hollister T, Delohery T, Hackett N, McMahill M, Sphicas E, Domingo D *et al*. A novel response of cancer cells to radiation involves autophagy and formation of acidic vesicles. Cancer Res 2001, 61: 439–444
18 Niemann A, Takatsuki A, Elsasser HP. The lysosomotropic agent monodansylcadaverine also acts as a solvent polarity probe. J Histochem Cytochem 2000, 48: 251–258
19 Mizushima N. Methods for monitoring autophagy. Int J Biochem Cell Biol 2004, 36: 2491–2502
20 Traganos F, Darzynkiewicz Z. Lysosomal proton pump activity: supravital cell staining with acridine orange differentiates leukocyte subpopulations. Methods Cell Biol 1994, 41: 185–194
21 Paglin S, Hollister T, Delohery T, Hackett N, McMahill M, Sphicas E, Domingo D *et al*. A novel response of cancer cells to radiation involves autophagy and formation of acidic vesicles. Cancer Res 2001, 61: 439–444
22 Kanzawa T, Kondo Y, Ito H, Kondo S, Germano I. Induction of autophagic cell death in malignant glioma cells by arsenic trioxide. Cancer Res 2003, 63: 2103–2108
23 Kanzawa T, Germano IM, Komata T, Ito H, Kondo Y, Kondo S. Role of autophagy in temozolomide-induced cytotoxicity for malignant glioma cells. Cell Death Differ 2004, 11: 448–457
24 Zeng X, Overmeyer JH, Maltese WA. Functional specificity of the mammalian Beclin-Vps34 PI 3-kinase complex in macroautophagy versus endocytosis and lysosomal enzyme trafficking. J Cell Sci 2006, 119: 259–270
25 Sherr CJ, McCormick F. The RB and p53 pathways in cancer. Cancer Cell 2002, 2: 103–112
26 Hofseth LJ, Hussain SP, Harris CC. p53: 25 years after its discovery. Trends Pharmacol Sci 2004, 25: 177–181
27 Joers A, Jaks V, Kase J, Toivo M. p53-dependent transcription can exhibit both on/off and graded response after genotoxic stress. Oncogene 2004, 23: 6175–6185
28 Yu J, Zhang L, Hwang PM, Kinzler KW, Vogelstein B. PUMA induces the rapid apoptosis of colorectal cancer cells. Mol Cell 2001, 7: 673–682
29 Nakano K, Vousden KH. PUMA, a novel proapoptotic gene, is induced by p53. Molecular Cell 2001, 7: 683–694
30 Yu J, Zhang L. No PUMA, no death: implications for p53-dependent apoptosis. Cancer Cell 2003, 4: 248–249
31 Edinger AL, Thompson CB. Death by design: apoptosis, necrosis and autophagy. Curr Opin Cell Biol 2004, 16: 663–669
32 Boya P, Gonzalez-Polo RA, Casares N, Perfettini JL, Dessen P, Larochette N, Metivier D *et al*. Inhibition of macroautophagy triggers apoptosis. Mol Cell Biol 2005, 25: 1025–1040
33 Kabeya Y, Mizushima N, Ueno T, Yamamoto A, Kirisako T, Noda T, Kominami E *et al*. LC3, a mammalian homologue of yeast Apg8p, is localized in autophagosome membranes after processing. EMBO J 2000, 19: 5720–5728
34 Feng Z, Zhang H, Levine AJ, Jin S. The coordinate regulation of the p53 and mTOR pathways in cells. Proc Natl Acad Sci USA 2005, 102: 8204–8209